*Astronomical and Astrophysical Transactions* (*AApTr*), 2019, Vol. 31, Issue 2, pp. 199–208,
ISSN 1055-6796, Photocopying permitted by license only, ©Cambridge Scientific Publishers

# A statistical study of linear jets in the low solar corona

I.P. Loboda*, S.A. Bogachev

*P.N. Lebedev Physical Institute, Russian Academy of Sciences, Moscow, Russia*

*Received 1 October, 2018*

In this work we studied the dynamics of linear jets in the low solar corona which follow parabolic trajectories off-limb in the He II 304 Å observations. We identified 338 such events and obtained their spatial and dynamic characteristics, including their lengths, lifetimes, initial velocities, and decelerations. These jets are characterized by the absence of lateral deflections and small widths, mean heights of 16–32 Mm, typical lifetimes of 13–18 min and initial velocities of 65–140 km/s. Moreover, a substantial fraction of the jets have decelerations larger than solar gravity, which, given no correlation with the inclinations, and a strong correlation of decelerations with initial velocities, allows us to propose a model of magneto-acoustic shocks for this kind of jets, that was successfully used to explain the dynamics of smaller chromospheric jets, such as spicules and dynamic fibrils. However, a much larger period of oscillations (10.3 min compared to 2.1 min) probably suggests a different formation mechanism.

*Keywords*: Sun: activity, Sun: corona, Sun: transition region, Sun: oscillations

## 1 Introduction

The solar atmosphere is populated by many types of jets, the smallest of which are spicules, which are observed in the chromosphere (Roberts 1945), and the largest are the coronal jets, observed correspondingly in the solar corona (Shibata et al. 1992). In-between there is a broad variety of jets observed in the transition-region spectral lines, such as He II 304 Å, which is formed at the temperature around $8 \times 10^4$ K. These jets are commonly termed macrospicules and were first observed during the Skylab mission (Bohlin et al. 1975).

However, because of such a definition, observations of macrospicules show a broad variation of their properties. They have heights from 7 to 70 Mm, maximum velocities from 10 to 150 km $s^{-1}$, and lifetimes from 3 to 45 min (Withbroe et al. 1976; Dere et al. 1989). Spectroscopic observations have detected Doppler shifts, which were interpreted as rotations of macrospicules (Scullion et al. 2009). On the other hand,

*Email: loboda@sci.lebedev.ru

several studies have observed the parabolic trajectories of these jets, which have decelerations smaller than free-fall acceleration near the surface of the Sun (Karovska and Habbal 1994). This behaviour was explained at that time by strong inclinations of macrospicules.

Jets of a similar size, which are observed in the H$\alpha$ spectral line and are probably the chromospheric counterparts of macrospicules, were later shown to consist of two groups with different morphology and dynamics (Wang 1998). Also, Georgakilas et al. (1999) have shown that macrospicules are different by their physical properties from polar surges – another type of solar jets of medium size. Furthermore, a clear boundary between macrospicules and coronal jets have not been established (Moore et al. 2013).

As a result, it is not understood whether there is a common physical mechanism that produces the macrospicules, and what this mechanism could be, although some attempts have been made to reproduce macrospicules with the help of numerical modelling (Murawski et al. 2011). It is also not clear whether macrospicules are the same phenomena as spicules, which occasionally can reach bigger heights because of a favourable combination of external conditions, or they have an essentially different mechanism of formation (Sterling 2000).

Several attempts have been recently made to make a statistical study of macrospicules (Bennett and Erdélyi 2015; Kiss et al. 2017) using the observations of the Atmospheric Imaging Assembly (AIA) which operated on the Solar Dynamics Observatory (SDO) satellite. However, these studies have defined macrospicules by a brightening in their base, and moreover, have artificially limited their heights and widths. This means that these authors could have included coronal jets as macrospicules, and therefore, their results can be subject to an observational bias. Taking into account all that has been said above, in this work we statistically studied the subclass of the linear jets, which follow parabolic trajectories to uncover their physical mechanism.

## 2 Observations and methods

For this purpose we used observations of the AIA on board the SDO in the He II 304 Å. This spectral line is excited at temperatures around $8 \times 10^4$ K, which corresponds to the transition region of the solar atmosphere. AIA observations of the full Sun are characterised by high angular and temporal resolution of $0.6''$ and 12 s respectively, and cover a period of more than eight years. In these data we selected 15 observation periods, each of which had a duration of 6 hours, therefore the total duration of our dataset is 90 hours which spans over the period from year 2010 to year 2015.

We identified the jets in these data using the synoptic maps of the limb, where our objects of interest are visible as straight and narrow areas of enhanced brightness. For each jet that we have identified, we constructed a map of maximum intensities that were observed throughout its lifetime; an example of one of these maps is shown in Fig. 1a. We used these maps to determine the axis of the jet, and consequently, to obtain its inclination and the position of its base on the limb. Instead of a heliographic latitude, the jet's position on the limb was defined by a polar angle counted in the clockwise direction from the nearest pole of the Sun.

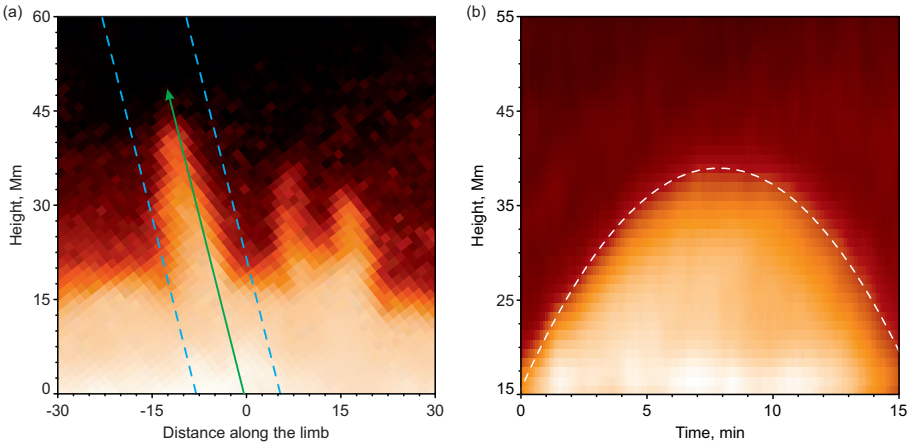



**Figure 1** The map of maximum intensities that are observed over the duration of a jet's motion in the He II 304 Å spectral line (a) and the time-distance map, which shows the dynamics of the jet along its inclined axis (b). In panel (a) the axis of the jet is shown with the green arrow, and the imaginary slit is shown there with the blue dashed lines. The approximated parabolic trajectory of the jet is shown in panel (b) with the white dashed curve.

To study the dynamics of the jet we surrounded it with an imaginary slit that is parallel to its axis and is wide enough to include all of the jet's material on the map of maximum intensities. We then summed the intensities in the horizontal direction and in this way we obtained the time-distance intensity maps, which reveal the axial dynamics of the jet. Also, because the jets are observed against a strong and inhomogeneous background, we subtracted from these maps the unperturbed vertical off-limb intensity profile in the He II 304 Å spectral line, which was additionally smoothed by a model function adopted from Loboda and Bogachev (2015). An example of the fully processed time-distance map is shown in Fig. 1b.

Using the time-distance maps we selected only those jets, which have both the ascending and descending phases of their motion, and moreover, follow parabolic trajectories with high precision. We approximated the trajectory of the selected jets with a second-order polynomial using the dynamic threshold method. The threshold, as well as the time interval of the fit were adjusted automatically based on the $\chi^2$ statistics. In this way the optimal parabolic approximation was found, from which we obtained the jet's maximal height, lifetime, initial velocity and deceleration.

## 3 Results of observations

With this method and data we identified 338 jets with parabolic trajectories and obtained their spatial and dynamic characteristics. The distributions of these parameters are shown in Fig. 2. We have found that the majority of these jets are concentrated around the solar pole, which shows that they are mostly located in the coronal holes (Fig. 2a). However, probably because the observations were made during

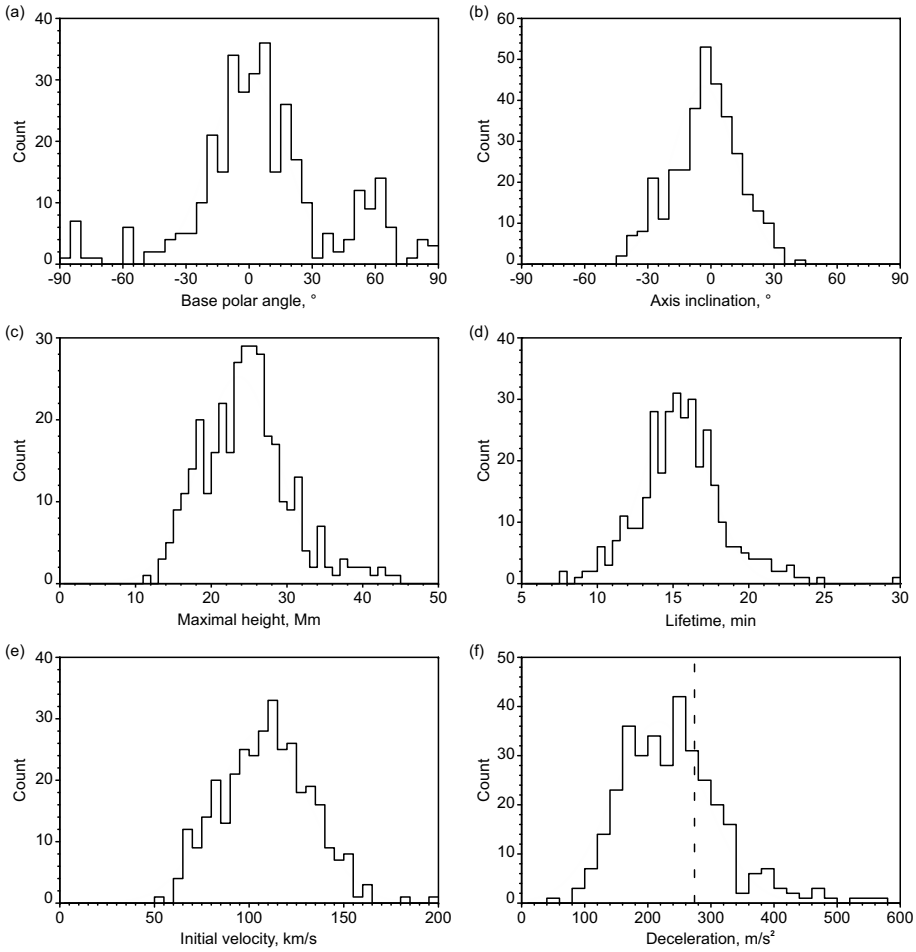



**Figure 2** Distribution of the jets by their location on the limb (a), axis inclination (b), maximal height (c), lifetime (d), initial velocity (e) and deceleration (f). Free-fall acceleration due to gravity on the Sun's surface is indicated in panel (f) with a dashed line.

the rising phase of the solar activity, a significant number of jets are also observed in the equatorial regions. We also found that all of the jets have visible inclinations less than 40° (Fig. 2b), which does not support the assumption of Karovska and Habbal (1994) that macrospicules can have inclinations larger than 65°.

We have found that the lengths of the majority of the jets are from 16 to 32 Mm (Fig. 2c). The peak of this distribution is significantly higher than the maximum height of spicules when they are observed in the He II 304 Å spectral line, which is equal in average to 10 Mm. From this we conclude that the linear jets, and consequently the macrospicueles, are not the statistical continuation of spicules. Also, these heights are smaller than those obtained by Bennett and Erdélyi (2015) and Kiss et al. (2017), which supports our assumptions that these studies could have included a certain fraction of larger jets as macrospicules. In our previous work such jets were

classified as polar surges because of their complex dynamics and morphology (Loboda and Bogachev 2017).

We have found that lifetimes are around 15 min (Fig. 2d), and the initial velocities are from 65 to 140 km/s (Fig. 2e). Both these values are close to the lifetimes and initial velocities of the so-called Type II spicules, which have been recently discovered (de Pontieu et al. 2007b). These spicules disappear fast from observations in the chromospheric spectral lines, but become visible in the transition-region spectral lines, such as He II 304 Å (Pereira et al. 2014). We therefore suggest that there can be in the least degree a partial correspondence between these two types of solar jets. Moreover, the initial velocities that we have obtained are close to the sound speed in the lower corona, which has the value of around 150 km/s.

The most interesting results, however, are given by the measurements of decelerations of the jets. Although the grater part of the jets have decelerations less than the free-fall acceleration due to gravity near the surface of the Sun, 36 % of the jets have decelerations larger than this value (Fig. 2f). Moreover, we have not found a non-negligible correlation between the inclinations of the jets and their decelerations. From this we can conclude that linear jets do not have free dynamics in the gravitational field of the sun, and an additional force is acting on them. In the physical conditions of the lower solar corona this force can be either the pressure gradient, the

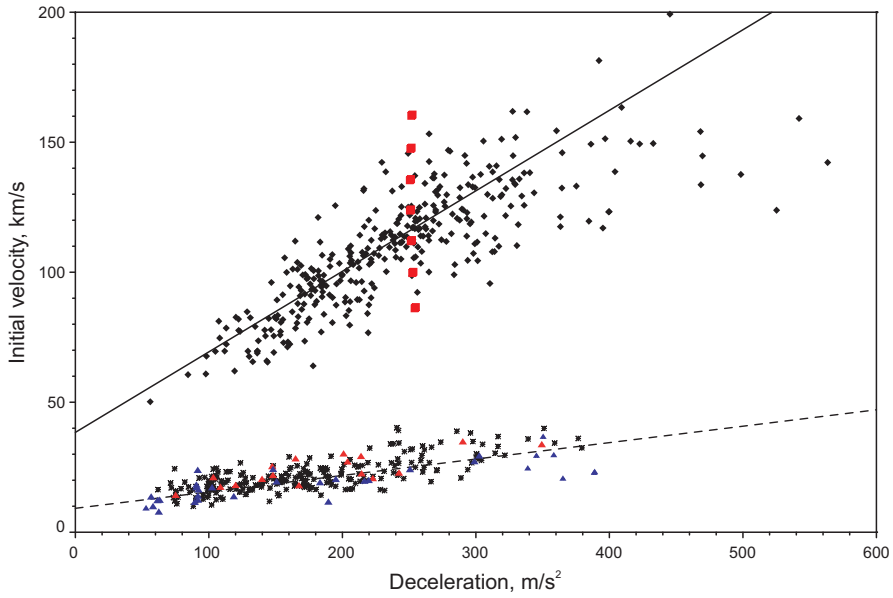



**Figure 3** Dependence of the initial velocities of the jets on their decelerations. The results of observations, which were obtained in this work, are shown with the black diamonds, and the results of numerical modelling are shown with the red square marks. For comparison, results in de Pontieu et al. (2007b) are shown: for type I spicules with the red triangles, for quiet-Sun mottles with the blue triangles, and for active-region fibrils with the black asterisks. The linear approximation for the results of observations in this work are shown with the solid black line, and for results in de Pontieu et al. (2007b) with the dashed black line.

magnetic tension force, or the magnetic pressure. This force, however, should have constant value in order to also result in the parabolic trajectory of the jet.

Moreover, we have found a strong correlation between the decelerations of the jets and their initial velocities (Fig. 3). This correlation has been previously discovered for several types of chromospheric jets, such as the the active-region fibrils, quiet-Sun mottles and ordinary, or type I spicules, all of which also have parabolic trajectories of their apexes (Hansteen et al. 2006; de Pontieu et al. 2007a,b; Rouppe van der Voort et al. 2007). It was shown that this behaviour is explained by the ascending propagation of the magneto-acoustic shock waves, which are excited by the photospheric oscillations. In this mechanism the plasma of the jet follows the linear velocity profile of the shock-wave, and in this way follows a parabolic trajectory.

It can be easily shown that in the above mechanism the initial, or maximal velocity of the jet, which is at the same time the amplitude of the shock-wave, is proportional to its deceleration, which is equal to the rate of the velocity change in the shock-wave. The coefficient of proportionality is consequently the semi-period of the shock-wave. Following these considerations, we have found that the period of the shocks that probably drive the linear transition-region jets is 10.3 min. This is sufficiently larger than the analogous period of the shock-waves for the chromospheric jets, which we calculated to be 2.1 min from the plots in the papers cited above. To demonstrate this difference we have added the results from de Pontieu et al. (2007b) to Fig. 3.

## 4 Results of numerical modelling

To check whether this mechanism can be reproduced numerically, we have performed the simulations using the Lare3d program package. This package is based upon the Lagrangian remap method, which provides the exact solution for the shock wave propagation process. As an initial condition we have used the realistic model of the solar atmosphere, which we adopted from Avrett and Loeser (2008) – an updated version of the widely used VAL III C model (Vernazza et al. 1981). To produce the jet in the stable atmosphere we have assigned a sinusoidal velocity disturbance on the photosphere.

By varying the amplitude of the initial disturbance from 10 to 40 km/s, we have calculated the formation and development of jets in the form of elevations of low-temperature and high-density chromospheric plasma into the corona, to the heights from 14.5 to 51 Mm. The space-time maps, which show the evolution of different physical parameters of plasma in one of the jets that we have calculated – the density, temperature, velocity (facing upwards) and pressure – are shown in Fig. 4. It is clearly seen that the jet has the precise parabolic trajectory, which is shown in all maps with a dashed curve.

By approximating the calculated trajectory of a jet with a second order polynomial in the same way as we have done previously for the jets in observations, we have obtained decelerations and initial velocities of the jets obtained in numerical modelling. We have added these values to Fig. 3 as red squares, and it can be clearly seen that, although the calculated jets have similar initial velocities and decelerations as the jets in observations, the numerical modelling does not reproduce the linear dependence that we have found in observations.

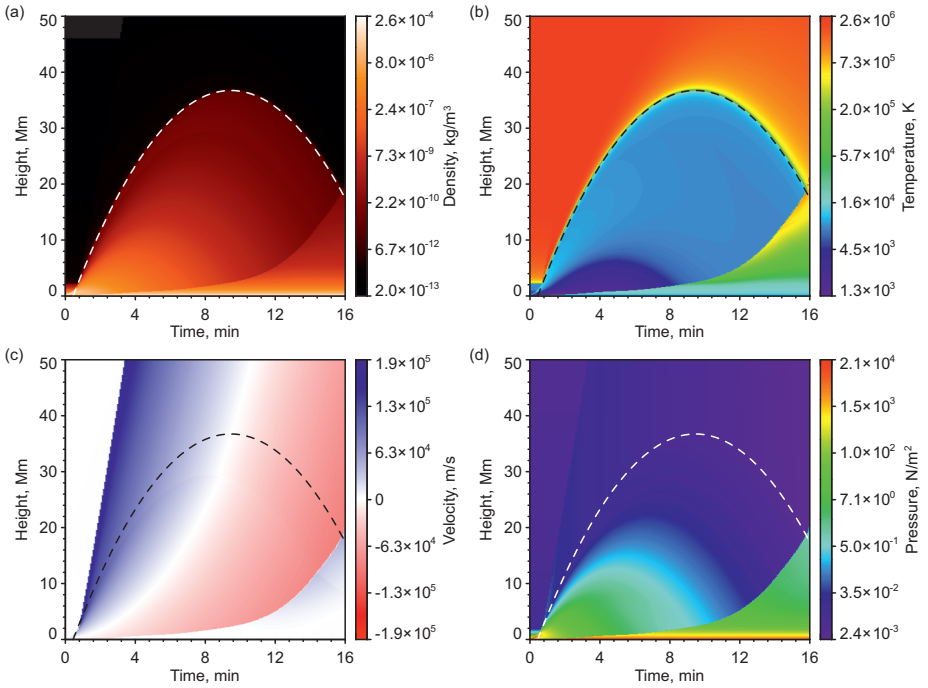



**Figure 4** Results of the one-dimensional numerical modelling of the jet. The figure shows the time-distance maps, which demonstrate the temporal evolution of the jet's plasma density (a), temperature (b), velocity (c) and pressure (d). The parabolic trajectory of the jet is shown in panels (a) and (d) with the white dashed line and in panels (b) and (c) with the black dashed line.

Furthermore, it can be seen in Fig. 4c that when the initial disturbance reaches the transition region it transforms into a shock wave. However, although the velocity profile of the shock wave is not linear the jet's apex still has the parabolic trajectory. This is an unexpected effect, which needs future theoretical explanation. Finally, Figure 4d shows an area of increased pressure in the lower part of the jet on the early stage of its motion, which allows us to conclude that the additional force that acts on the plasma of the jet is the pressure gradient. This means that the mechanism of the linear jets that we study in this work is not magnetic, but purely hydrodynamical.

## Conclusions

We have found that the dynamical mechanism of the linear jets in the lower corona are, with a high degree of probability, the same as the mechanism of chromospheric jets, including the type I spicules. However, the period of the magneto-acoustic shock waves are significantly higher in the case of linear jets that in the case of spicules, which shows that they are subjected to different formation conditions. We have also shown that the linear jets, which are visible in the transition region spectral lines, such as He II 304 Å, can be the the same physical structures as the type II spicules,

which disappear from the chromospheric spectral lines, probably because they are heated to higher temperatures.

We have also attempted to reproduce the jets that we have observed with the help of numerical modelling. By doing this, we could calculate the formation of jets of the same size. The calculated evolution of plasma velocity in the jet and the surrounding medium shows that a shock-wave is formed, which supports the mechanism, that we have proposed to explain the formation of linear jets in the low solar corona. However, we could not reproduce the linear dependence between the initial velocities of the jets and their deceleration, which shows that the model needs to be further developed in order to explain the mechanism of formation of the linear jets to the full extent.

## Acknowledgements

We acknowledge support from the Russian Science Foundation (grant 17-12-01567). In this work we used the observations of the AIA/SDO, and the Lare3d program package for numerical modelling.

## References

Avrett, E.H., Loeser, R. (2008) ApJS 175 229
Bennett, S.M., Erdélyi, R. (2015) ApJ 808 135
Bohlin, J.D., Vogel, S.N., Purcell, J.D. et al. (1975) ApJL 197 L133
de Pontieu, B., Hansteen, V.H., Rouppe van der Voort, L., van Noort, M., Carlsson, M. (2007a) ApJ 655 624
de Pontieu, B., McIntosh, S., Hansteen, V.H. et al. (2007b) PASJ 59 S655
Dere, K.P., Bartoe, J.D.F., Brueckner, G.E., Cook, J.W., Socker, D.G. (1989) SolPhys 119 55
Georgakilas, A.A., Koutchmy, S., Alissandrakis, C.E. (1999) A&A 341 610
Hansteen, V.H., De Pontieu, B., Rouppe van der Voort, L., van Noort, M., Carlsson, M. (2006) ApJL 647 L73
Karovska, M., Habbal, S.R. (1994) ApJL 431 L59
Kiss, T.S., Gyenge, N., Erdélyi, R. (2017) ApJ 835 47
Loboda, I.P., Bogachev, S.A. (2015) SolPhys 290 1963
Loboda, I.P., Bogachev, S.A. (2017) A&A 597 A78
Moore, R.L., Sterling, A.C., Falconer, D.A., Robe, D. (2013) ApJ 769 134
Murawski, K., Srivastava, A.K., Zaqarashvili, T.V. (2011) A&A 535 A58
Pereira, T.M.D., De Pontieu, B., Carlsson, M. et al. (2014) ApJL 792 L15
Roberts, W.O. (1945) ApJ 101 136
Rouppe van der Voort, L.H.M., De Pontieu, B., Hansteen, V.H., Carlsson, M., van Noort, M. (2007) ApJL 660 L169
Scullion, E., Popescu, M.D., Banerjee, D., Doyle, J.G., Erdélyi, R. (2009) ApJ 704 1385
Shibata, K., Ishido, Y., Acton, L.W. et al. (1992) PASJ 44 L173
Sterling, A.C. (2000) SolPhys 196 79
Vernazza, J.E., Avrett, E.H., Loeser, R. (1981) ApJS 45 635

Wang, H. (1998) ApJ 509 461
Withbroe, G.L., Jaffe, D.T., Foukal, P.V. et al. (1976) ApJ 203 528